



# Fermi $\gamma$ -ray ‘bubbles’ from stochastic acceleration of electrons

Philipp Mertsch and Subir Sarkar

Rudolf Peierls Centre for Theoretical Physics, University of Oxford, Oxford OX1 3NP, UK  
e-mail: p.mertsch@physics.ox.ac.uk

**Abstract.** Gamma-ray data from the Fermi-LAT show a bi-lobular structure extending up to 50 degrees above and below the Galactic centre, coincident with a possibly related structure in the ROSAT X-ray map. It has been argued that the  $\gamma$ -rays arise due to inverse Compton scattering of relativistic electrons accelerated at plasma shocks present in the bubbles. We explore the alternative possibility that the relativistic electrons undergo stochastic 2nd-order Fermi acceleration in the entire volume of the bubbles by plasma wave turbulence. This turbulence is generated behind the outer shock and propagates into the bubble volume, leading to a non-trivial spatial variation of the electron spectral index. Rather than a constant volume emissivity as predicted in other models we find an almost constant surface brightness in  $\gamma$ -rays and also reproduce the observed sharp edges of the bubbles. We comment on possible cross-checks in other channels.

**Key words.**  $\gamma$ -ray sources, galactic diffuse emission, acceleration of cosmic rays

## 1. Introduction

Recently, data from the Fermi-LAT have revealed (Su et al. 2010) the presence of two huge bi-lobular structures in  $\gamma$ -rays, the so-called “Fermi bubbles”, extending up to  $50^\circ$  above and below the galactic plane. The overall spectrum of the bubbles is  $\propto E^{-2}$ , i.e. much harder than the  $\pi^0$ , inverse Compton (IC) and bremsstrahlung foregrounds from galactic cosmic rays in the disk, and extends from a spectral shoulder at about a GeV up to a cut-off/roll-over at a few hundreds of GeV. The bubbles have an almost constant surface brightness with sharp edges. The above properties as well as the size and position of the bubbles are rather robust with respect to the details of foreground subtraction making it unlikely that the bubbles are an artefact of the foreground subtraction.

Both the position at galactic longitude  $\ell = 0^\circ$  and its symmetry with respect to the galactic plane hint at the galactic centre (GC) as the origin of the bubbles. While similar structures have been observed in radio galaxies the detection of the Fermi bubbles is puzzling given that there is no evidence for present activity of the massive black hole at the GC. Data from the ROSAT X-ray satellite (Snowden et al. 1997) show evidence for a limb brightened structure coinciding with the bubble edges, possibly from a shock front. The non-observation of X-rays from the bubble interior, on the other hand, points at a relatively thin, hot plasma. With estimates for a gas density of  $n \sim 10^{-2} \text{ cm}^{-3}$  and a temperature of  $T \sim 2 \text{ keV}$ , the total energy in hot gas is  $\sim 10^{54-55} \text{ erg}$  (Su et al. 2010). Furthermore, assuming velocities typical for shock fronts in the interstellar medium

gives  $\sim 10^7(U/1000 \text{ km s}^{-1})\text{yr}$  for the age of the bubbles at a projected distance of 10 kpc.

While we choose to remain agnostic about the origin of the bubbles itself we note that a shock might have been produced by a jet active for a few million years. It has recently been shown (Guo & Mathews 2011) that a light but overpressured jet powered by  $\sim 10\%$  of the Eddington luminosity leads to a shock coincident with the bubble edge and in agreement with the overall bubble shape. In the following, we will explain the non-thermal emission from the bubbles by 2nd-order Fermi acceleration of electrons and IC scattering of these electrons on ambient radiation fields. As the electrons are constantly accelerated in the whole bubble this can lead to the hard  $\gamma$ -ray spectrum.

## 2. Second order Fermi acceleration

In particular, we start from the evidence for a shock front from ROSAT. At the outer shock, Rayleigh-Taylor and Kelvin-Helmholtz instabilities will generate plasma turbulence that is then being convected into the bubble interior by the downstream bulk flow. The turbulence will cascade from the injection scale  $L$  to smaller scales and will finally be damped at a scale  $l_d$ , i.e. once the kinetic energy of the turbulence becomes comparable to the magnetic field energy,  $v_{\text{edd}}(l_d) \approx v_A$ . The usual Rankine-Hugoniot conditions allow to compute (Fan et al. 2009) the spatial variation of the eddy velocity at the injection scale,  $u$ , and the magnetosonic phase velocity,  $v_F$ , with distance  $x = \xi L$  from the shock:

$$u(\xi) = \frac{U}{4} \frac{1}{C_1 \xi/3 + a^{-1/2}}, \quad (1)$$

$$v_F(\xi) = \frac{U}{4} \left( 5 - \frac{5}{3(C_1 \xi/3)^2} + 4 \frac{v_A^2}{U^2} \right)^{1/2}, \quad (2)$$

where  $U$  is the shock velocity,  $v_A$  the Alfvén velocity (which we assume to be constant and equal to the speed of sound  $v_{s,0}$  at the shock) and  $a = 3 - 16v_{s,0}^2/U^2$ .

We consider the stochastic acceleration by large-scale, fast mode turbulence (Ptuskin 1988). Second order Fermi acceleration processes like this have been proven successful

in explaining the non-thermal spectra of high-energy electrons in a variety of astrophysical environments (Scott & Chevalier 1975; Lacombe 1977; Achterberg 1979; Eilek 1979; Cowsik & Sarkar 1984; Fan et al. 2009) and might be responsible for the acceleration of ultra-high energy cosmic rays (Hardcastle et al. 2008; O’Sullivan et al. 2009). The spectrum is governed by the Fokker-Planck equation,

$$\frac{\partial n}{\partial t} - \frac{\partial}{\partial p} \left( p^2 D_{pp} \frac{\partial n}{\partial p} \right) - \frac{n}{t_{\text{esc}}} + \frac{\partial}{\partial p} \left( \frac{dp}{dt} n \right) = 0, \quad (3)$$

where  $n(p, t) dp$  is the density of electrons with momentum in  $[p, p + dp]$ . The second, third and fourth term describe diffusion and systematic gains in momentum, escape due to spatial diffusion and energy losses by synchrotron radiation and IC scattering (with cooling time  $t_{\text{cool}} \sim p/(dp/dt)$ ), respectively. The diffusion coefficient in momentum for scattering by fast magnetosonic waves is (Ptuskin 1988)

$$D_{pp} = p^2 \frac{8\pi D_{xx}}{9} \int_{1/L}^{k_d} dk \frac{W(k)k^4}{v_F^2 + D_{xx}^2 k^2}, \quad (4)$$

where  $D_{xx}$  is the spatial diffusion coefficient and  $W(k)$  is the turbulence spectrum. This translates into the timescale for acceleration,  $t_{\text{acc}} \sim p^2/D_{pp}$ .

Both  $t_{\text{acc}}$  and  $t_{\text{esc}}$  (and therefore the resulting spectrum) depend on three parameters that cannot be inferred directly from observations. The scale of turbulence injection  $L$  is necessarily smaller than the size of the bubbles and MHD simulations show generation of turbulence on kiloparsec scales. Here, we assume  $L = 2 \text{ kpc}$ . The shock velocity can in principle be determined from the displacement of the shock; the shock needs  $\sim 50(U/10^8 \text{ cm s}^{-1})^{-1} \text{ yr}$  to move a distance corresponding to the  $1''$  resolution of the Chandra X-ray observatory. Here, we fix  $U = 2.6 \times 10^8 \text{ cm s}^{-1}$ , a value consistent with MHD simulations (Guo & Mathews 2011). Finally the normalised Alfvén velocity is given by the square root of twice the ratio of the magnetic field energy density to thermal plasma energy density:  $\beta_A = v_A/c = \sqrt{2U_B/U_\rho}$ . Hence  $\beta_A \gtrsim 2.8 \times 10^{-4}$  for an estimated upper limit on the thermal gas density  $n \lesssim 10^{-2} \text{ cm}^{-3}$  (Su et al.

2010) and a magnetic field  $B = 4 \mu\text{G}$ . Such a field strength in the halo is suggested by radio observations of edge-on spiral galaxies as NGC 891 (Beck et al. 1979). Here we adopt  $\beta_A = 5 \times 10^{-4}$ .

With these adopted parameters  $l_d > 8 \times 10^{19} (L/\text{kpc})(U/10^8 \text{ cm s}^{-1})^{-3} (\beta_A/10^{-3})^3 \text{ cm}$  is always larger than the gyro-radius of electrons  $\sim 7.5 \times 10^{11} (B/4 \mu\text{G})^{-1} (E/\text{GeV}) \text{ cm}$ . Hence, the spatial diffusion coefficient and also the escape and acceleration times are energy-independent. Furthermore, with the parameters as above we recover a hierarchy of timescales,  $t_{\text{acc}}, t_{\text{esc}} \ll t_{\text{life}}$  which justifies the use of the steady state solution (Stawarz & Petrosian 2008),

$$n(p) \propto \begin{cases} p^{-\sigma} & \text{for } p \ll p_{\text{eq}}, \\ p^2 e^{-p/p_{\text{eq}}} & \text{for } p \sim p_{\text{eq}}, \end{cases} \quad (5)$$

with  $p_{\text{eq}}$  defined by  $t_{\text{acc}}(p_{\text{eq}}) \equiv t_{\text{cool}}(p_{\text{eq}})$ . The spectral index,  $-\sigma = 1/2 - \sqrt{9/4 + t_{\text{acc}}/t_{\text{esc}}}$ , is determined by the ratio of acceleration and escape times alone and asymptotically approaches  $-1$  as  $t_{\text{acc}}/t_{\text{esc}} \rightarrow 0$ . One could argue that for low energies the cooling time becomes larger than the dynamical time scale  $t_{\text{life}}$  and that therefore the use of the steady state solution is not strictly justified. However, it has been shown (Becker et al. 2006) for 2nd-order Fermi acceleration that irrespective of the loss rate the spectrum always attains the steady state spectrum in a few times  $t_{\text{acc}}$  and that the steady state solution can therefore be applied as long as  $t_{\text{acc}} \ll t_{\text{life}}$ . The change in timescales  $t_{\text{acc}}$  and  $t_{\text{esc}}$  with distance from the shock front  $\xi$  (through  $u(\xi)$  and  $v_F(\xi)$ ) is therefore adiabatic such that the electron spectrum relax quickly to its steady state value.

The emissivity in  $\gamma$ -rays is calculated in the most general form (Blumenthal & Gould 1970) using a recent model of interstellar radiation fields (Porter & Strong 2005) and depends on the distance from the shock. We calculate the flux of photons by integrating along the line of sight through the bubble. The overall normalisation of the electron spectrum depends on the efficiency of injection, which we fix by demanding that our model matches the total  $\gamma$ -ray flux? Integration of

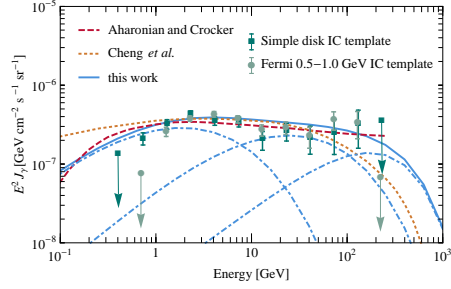


**Fig. 1.** The overall spectrum  $E^2 J_\gamma$  in  $\gamma$ -rays. The data are shown as obtained with two different IC templates (Su et al. 2010). The fits from a hadronic (Crocker & Aharonian 2010) and a leptonic (Cheng et al. 2011) model are shown by the dashed and dotted lines, respectively. The  $\gamma$ -ray flux from our model is shown by the solid line and the dot-dashed lines show the contributions from IC scattering on the CMB, FIR and optical/UV (from left to right).

the (position-dependent) spectrum over both bubbles shows that the total energy in electrons above 100 MeV is  $\sim 10^{51} \text{ erg}$ . This is a rather moderate energy demand, in particular in comparison to the hadronic model (Crocker & Aharonian 2010) which requires up to five orders of magnitude more energy in high energy protons.

### 3. Results

The overall spectrum of  $\gamma$ -rays from the bubbles is shown in Fig. 1 and compared to the data and predictions from other models. Our model not only reproduces the  $E^{-2}$  spectrum but also both the spectral shoulder around 1 GeV and the roll-over/cut-off at  $\sim 200 \text{ GeV}$ . We note that the other two models presented would need to invoke a somewhat unmotivated break in the proton/electron spectrum to produce *both* features whereas in our model they arise naturally due to the very hard electron spectrum and the cut-off due to cooling.

In Fig. 2, we compare the data with the intensity as a function of distance from the bubble edge predicted by our model and obtained in the same fashion as in Su et al. (2010), i.e. averaging over great circles intersecting the

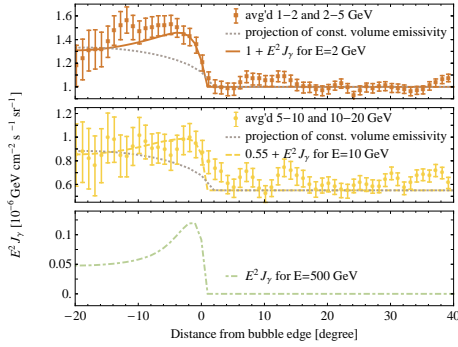


**Fig. 2.** The intensity  $E^2 J_\gamma$  in  $\gamma$ -rays is shown as a function of the distance from the bubble edge at 2 GeV (solid line), 10 GeV (dashed line) and 500 GeV (dot-dashed line), together with the data (Su et al. 2010) from the averaged 1 – 2 and 2 – 5 GeV and the averaged 5 – 10 and 10 – 20 GeV maps. We also show the profile expected from a constant volume emissivity (dotted line) which clearly does not reproduce the observed profile.

bubble centre. At both energies for which data is available (2 and 10 GeV) our model nicely reproduces the constant profile inside the bubbles and their sharp edges, i.e. the jump in intensity within a few degrees around the bubble edges. We have also computed the profile at 500 GeV which is much more limb-brightened – a robust prediction of our model. We note that the profile expected from a constant volume emissivity, as predicted by a hadronic (Crocker & Aharonian 2010) and a leptonic (Cheng et al. 2011) model, would be much softer at the edges and does not reproduce the data.

While the “WMAP haze” (Finkbeiner 2004) has not been observed in polarised emission (Gold et al. 2010) and may be just an artefact of the template subtraction (Mertsch & Sarkar 2010), it has been proposed as a physical counterpart of the Fermi bubbles (Su et al. 2010). However, in our model the expected synchrotron flux in the middle of the bubble is of the required amplitude *only* if the magnetic field is as strong as  $15 \mu\text{G}$ . For a  $4 \mu\text{G}$  field the synchrotron flux is significantly lower,  $1.6 \times 10^{-21} (\nu/\text{GHz})^{-0.2} \text{ erg cm}^{-2} \text{ s}^{-1} \text{ sr}^{-1}$ . The hadronic model predicts a detectable flux

of neutrinos for the proposed Mediterranean  $\text{km}^3$  neutrino telescope (Crocker & Aharonian 2010). We stress however that the observed bubble profile already disfavors this model (as well as the leptonic DSA model) and instead favours our model with 2nd-order Fermi acceleration of electrons.

## References

- Achterberg, A., 1979, *Astron. Astrophys.*, 76, 276  
 Beck, R., et al., 1979, *Astron. Astrophys.*, 77, 25.  
 Becker, P.A., et al., 2006, *Astrophys. J.*, 647, 539  
 Blumenthal, G.R., & Gould, R.J., 1970, *Rev. Mod. Phys.*, 42, 237  
 Cheng, K.S., et al., [2011 *ApJ* 731 L17].  
 Cowsik, R., & Sarkar, S., 1984, *Mon. Not. R. Astron. Soc.*, 207, 745  
 Crocker, R.M., & Aharonian, F., 2011, *Phys. Rev. Lett.*, 106, 101102.  
 Eilek, J.A., 1979, *Astrophys. J.* 230, 373  
 Fan, Z., et al., 2009, *Mon. Not. R. Astron. Soc.*, 406, 1337  
 Finkbeiner, D.P., [astro-ph/0409027].  
 Gold, D.P., et al., 2011, *Astrophys. J. Suppl.*, 192, 15.  
 Guo, F., & Mathews, W.G., [arXiv:1103.0055].  
 Hardcastle, M.J., et al., 2009, *Mon. Not. R. Astron. Soc.*, 393, 1041  
 Lacombe, C., 1977, *Astron. Astrophys.*, 54, 1  
 Mertsch, P., & Sarkar, S., 2010, *JCAP*, 1010, 019  
 O’Sullivan, S., et al., 2009, *Mon. Not. R. Astron. Soc.*, 400, 248  
 Porter, T.A., & Strong, A.W., *Proc. 29th Int. Cosmic Ray Conf.*, Pune, 2005, 4, 77  
 Ptuskin, V.S., 1988, *Sov. Astron. Lett.*, 14, 255  
 Scott, J.S., & Chevalier, R.A., 1975, *Astrophys. J. Lett.*, 197, L5  
 Snowden, S.L., et al., 1997, *Astrophys. J.*, 485, 125  
 Stawarz, L., & Petrosian, V., 2008, *Astrophys. J.*, 681, 1725  
 Su, M., et al., 2010, *Astrophys. J.*, 724, 1044